JOURNAL OF AIRCRAFT
Vol. 42, No. 6, November–December 2005

Identification of Experimental Unsteady Aerodynamic Impulse Responses

Walter A. Silva,* David J. Piatak,† and Robert C. Scott‡
NASA Langley Research Center, Hampton, Virginia 23681-0001

The identification of experimental unsteady aerodynamic impulse responses using the Oscillating Turntable (OTT) at NASA Langley's Transonic Dynamics Tunnel is described. Results are presented for two configurations: a rigid semispan model and a rectangular wing with a supercritical airfoil section. Both models were used to acquire unsteady pressure data caused by pitching oscillations on the OTT. A deconvolution scheme involving a step input in pitch and the resultant step response in pressure, for several pressure transducers, is used to identify the pressure impulse responses. The identified impulse responses are then used to predict the pressure response caused by pitching oscillations at several frequencies. Comparisons with the experimental data are presented.

Introduction

COMPLEX flight dynamic and aeroelastic phenomena are best understood by studying the underlying unsteady aerodynamic behavior. To this end, experiments designed to measure the unsteady aerodynamic response of various configurations provide significant and valuable information.[1–4] Experimental results are compared to various types of numerical analyses [such as computational fluid dynamics (CFD)] to provide insight into the underlying physics of the problem.

Insight gained from unsteady aerodynamic experiments and analyses can then be used to alter or control some aspect of the underlying physics leading to a modification of the performance of a vehicle. This is the primary goal of the flow-control research effort.[5–8] A thorough understanding of the dominant flow physics can lead to an optimal flow-control strategy. Therefore, understanding unsteady aerodynamic behavior is an essential step in the design of flow-control concepts as well.

For computational methods, the development of reduced-order models (ROM) has proven beneficial toward understanding dominant flow physics.[9,10] These methods provide insight regarding the level of nonlinearity within a physical process including nonlinear aeroelastic responses and aeroelastic limit-cycle oscillations (LCO). In previous work, aerodynamic impulse responses are numerically identified and used to provide insight into the dominant flow physics. These aerodynamic impulse responses are then used to develop computationally efficient state-space models of the aeroelastic system.

The measurement of unsteady aerodynamic and aeroelastic data is essential to the understanding of the flow physics and structural dynamics that govern a particular experiment. The analysis and interpretation of this type of data, however, are typically hampered by two complications: 1) a wide range of behavior that is difficult to classify as either linear or nonlinear and 2) noise in the data. The method presented herein targets these complications directly. Although the results presented are for unsteady aerodynamic pressures, the method can be applied to unsteady aerodynamic and aeroelastic loads as well.

The goals of this paper are 1) to demonstrate the feasibility of identifying unsteady aerodynamic impulse responses from experimental unsteady aerodynamic measurements and 2) to investigate the filtering capability of the methodology used to generate the aerodynamic impulse responses. The identification of the unsteady aerodynamic impulse responses will provide a direct method for evaluating the linearity (or nonlinearity) of any response. This evaluation is performed by comparing the predicted response using a linearized impulse response with the measured response. The level of correlation between the two responses (predicted vs measured) can be used to define linear and nonlinear regions of response. In addition, the use of a deconvolution technique will provide valuable filtering of the data above and beyond that of standard filters. That is, deconvolution, by definition, generates an impulse response via the correlation of an input/output pair. Data that are not input/output correlated are automatically filtered from the creation of the impulse response. Therefore, any uncorrelated white noise that might be present in the measurements will be filtered out via the deconvolution procedure. Note that this filtering capability will not be based on a given frequency range (low-pass, high-pass, or bandpass) but rather on the correlation of the input/output measurements.

Oscillating Turntable

The Oscillating Turntable (OTT) is a unique research tool at the Transonic Dynamics Tunnel (TDT) that provides the ability to oscillate relatively large, semispan wind-tunnel models in pitch at frequencies up to 40 Hz. This research tool has been designed specifically for the acquisition of unsteady pressure and loads data on rigid wind-tunnel models in order to study flow phenomena associated with flutter, LCO, shock dynamics, and nonlinear unsteady aerodynamic effects on a wide variety of aerospace vehicle configurations at transonic speeds.[2] Models can be oscillated sinusoidally at constant or varying frequencies, be subjected to a step input, or undergo user-defined motions. It is anticipated that unsteady pressure measurements caused by precisely controlled model motions will provide valuable data for CFD correlation and aircraft design with respect to unsteady aerodynamic/aeroelastic phenomena.

Rigid Semispan Model

Figure 1 shows the planform layout and main components of the rigid semispan model (RSM) including the OTT mount. The RSM planform is a 1/12th-scale configuration based on an early design known as the Reference H configuration that was a component of the High Speed Research program.[4] Model airfoil shapes were based on those of the Reference H configuration, with the model wing thickness being increased to a constant 4% thickness-to-chord ratio in order to accommodate pressure instrumentation at the wing tip. The model was designed to be very stiff to allow the measurement of aerodynamic properties with only negligible effects of structural deformations.

Presented as Paper 2003-1959 at the Structures, Structural Dynamics, and Materials Conference, Norfolk, VA, 7–10 April 2003; received 31 August 2004; revision received 24 February 2005; accepted for publication 24 February 2005.

*Senior Research Scientist, Aeroelasticity Branch.
†Aerospace Engineer, Aeroelasticity Branch.
‡Senior Aerospace Engineer, Aeroelasticity Branch.

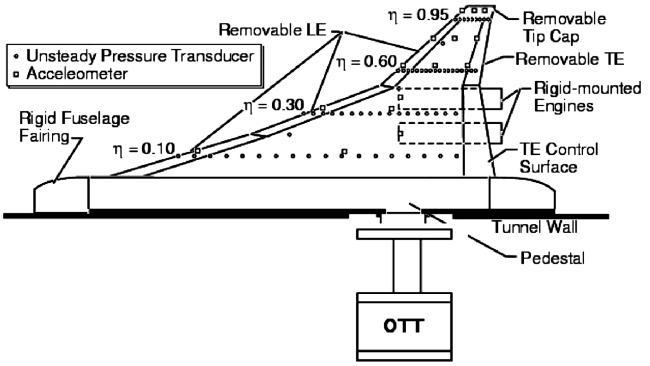

Fig. 1 Planform, model details, and instrumentation layout for the RSM wind-tunnel model.

The RSM was tested with a rigid fuselage fairing, which displaced the model away from the wind-tunnel wall boundary layer while serving as an aerodynamic boundary condition at the wing root. Additionally, the rigid fuselage fairing provided an aerodynamic shield for the hardware, instrumentation, and wire bundles located at the wing root. Two different fuselages were used with the RSM. A long fuselage fairing was used when it was tested on the balance, and a shorter fuselage fairing was used when it was tested on the OTT.

The instrumentation layout for the RSM (visible in Fig. 1) consisted of 131 in situ unsteady pressure transducers located at the 10, 30, 60, and 95% span stations. An attempt to capture broad spanwise effects was provided with the installation of six additional unsteady pressure transducers installed at the 20% chord station for the 20, 45, and 75% span stations for both upper and lower surfaces. Channels were carved into the foam core to accommodate the wiring for the instrumentation. Instrumentation also included accelerometers installed throughout the wing. The fuselage fairing used for testing the RSM on the OTT was instrumented with unsteady pressure transducers.

Benchmark Supercritical Wing

The benchmark supercritical wing (BSCW) has a rectangular planform with a 32-in. span, 16-in. chord, and a NASA SC(2)-0414 airfoil. Using 40 in situ transducers, unsteady pressure measurements were made along the chord at the 60% spanwise location at Mach numbers ranging from 0.4 to 0.85 and dynamic pressures of 100, 170, and 200 psf in R-134a heavy gas. Reynolds numbers based on model chord ranged from 2.4 to 6.5×10^6, and these test conditions corresponded to reduced frequencies k from 0.011 to 0.579 for the BSCW. Boundary-layer transition was fixed at 7.5% chord, and the OTT pitch axis was located at $x/c = 0.3$. The BSCW model has been previously tested at the TDT as part of the Benchmark Models Program.[11,12] during which a large database of unsteady pressures were obtained during motions on a flexible pitch and plunge mount.

Methodology

Unsteady pressure measurements were made on the RSM and the BSCW while the models underwent pitch oscillations on the OTT at frequencies from 1 to 10 Hz (RSM) and from 1 to 30 Hz (BSCW). The selection of these frequencies was based on the limitations of the OTT given the size of the wings. For the RSM with a large pitch inertia, 10 Hz was the maximum safe operational frequency that could be realized by the OTT. For the BSCW with a much smaller pitch inertia, frequencies of up to 30 Hz were attainable. In addition, unsteady pressures were acquired during RSM/OTT and BSCW/OTT step inputs in order to provide data to compute aerodynamic impulse responses.

The identification of aerodynamic impulse responses can be performed using system-identification techniques. The computational identification of unsteady aerodynamic impulse responses in order to develop efficient CFD-based models for aeroelastic analyses has recently been performed.[10] These efficient computational models are known as ROMs and comprise one aspect of a very active research effort at several research organizations.[9]

The identification of experimental unsteady aerodynamic (pressure) ROMs can be performed by using the same techniques used to identify the computational unsteady aerodynamic ROMs. The Volterra theory of nonlinear systems is used as the basis for modeling the linear and nonlinear dynamic response of the unsteady aerodynamic system under investigation. The basic premise of the Volterra theory is that the response of a nonlinear system to an arbitrary input can be approximated by the infinite sum of multidimensional convolution integrals

$$\begin{aligned} \boldsymbol{y}(t) &= \int_0^t \boldsymbol{h}_1(t-\tau)u(\tau)\,\mathrm{d}\tau \\ &\quad + \int_0^t \int_0^t \boldsymbol{h}_2(t-\tau_1, t-\tau_2)u(\tau_1)u(\tau_2)\,\mathrm{d}\tau_1\,\mathrm{d}\tau_2 \\ &\quad + \sum_{n=3}^{N} \int_0^t \cdots \int_0^t \boldsymbol{h}_n(t-\tau_1, \ldots, t-\tau_n) \\ &\quad \times u(\tau_1)\ldots u(\tau_n)\,\mathrm{d}\tau_1 \ldots \mathrm{d}\tau_n \end{aligned} \tag{1}$$

The kernels $(h_1, h_2, \ldots)$ represent various linear and nonlinear levels of the dynamics of the system. The first-order kernel h_1 is the linear (or linearized) impulse response and the higher-order kernels (h_2 and higher) represent second-order nonlinear impulse responses, third-order nonlinear impulse responses, and so on.

For the present study, the identification of experimental unsteady aerodynamic impulse responses will be limited to the first-order, or linearized, kernel. It is referred to as a linearized kernel because identification of the kernel (impulse response) can occur about a nonlinear steady-state condition (such as a transonic Mach number). First-, second-, and third-order kernels have been successfully identified for various nonlinear aeroelastic systems (computationally and experimentally) described in the references.[13] Future research will focus on the identification of the higher-order kernels for unsteady pressure measurements. The frequency-domain version of the second-order kernel is known as the bispectra, which has found important applications across a wide variety of disciplines for quantifying experimental nonlinear dynamics. [14]

The identification of the experimental unsteady aerodynamic impulse responses (first-order kernel) will consist of the deconvolution of a given input/output pair. Deconvolution involves the extraction of the impulse response of a system when the input and corresponding output are known. The input, in this case, is a sequence of positive and negative step inputs in pitch applied using the OTT, and the output is any of several measured pressure responses from the wind-tunnel models. Specifically, the input consists of a step change in angle of attack to five deg, which is held for 5 s, followed by a step change in angle of attack back to zero deg, held for 5 s, followed by a step change in angle of attack to negative 5 deg, held for 5 s, ending with a step change back to zero deg. The same input is used for all of the results presented in a subsequent section. Deconvolution is then used to extract the impulse response for the given input/output pair. For the given OTT step input, an impulse response can be identified for each pressure measurement (sensor) on the wind-tunnel models.

Direct prediction of the unsteady pressure response using a single step input (without deconvolution) would be problematic. This prediction requires convolution of the step response with the derivative of the input. Therefore, the derivative of a noisy signal would have to be computed, resulting in an even noisier signal. In addition, a single step input would be inadequate as only a specific angle-of-attack range (either positive or negative) would be excited. For a nonsymmetric airfoil such as that on the RSM and the BSCW, the application of a positive five-deg-angle-of-attack step followed by a negative five-deg-angle-of-attack step provides excitation for the entire five-deg positive and negative angle-of-attack range. Deconvolution using the measured (actual) input is then used to extract a single impulse response that is valid for the positive and negative five-deg-angle-of-attack range. In addition, the use of a deconvolution scheme yields valuable filtering properties.

Once the impulse response has been generated, convolution is used to predict the pressure response caused by sinusoidal inputs in pitch at various frequencies. The measured results are compared to the predicted results (via convolution) in the next section.

RSM/OTT Results

Results for the RSM/OTT are presented in this section. The RSM has a total of 131 in situ pressure transducers. A step input in pitch using the OTT results in 131 unsteady pressure responses. Therefore, deconvolution can be applied to all of the unsteady pressure measurements to yield 131 unsteady aerodynamic impulse responses. For the sake of brevity and to demonstrate the feasibility of the method, results are presented for only one pressure measurement located on the upper surface of the RSM at the 30% span location and the 20% chord station. The data were acquired at a Mach number M of 0.9, a dynamic pressure q of 150 psf, and with the RSM at zero-deg angle of attack. The data for these tests were acquired at 500 samples/s with an antialiasing filter at 200 Hz.

Figure 2 presents the step pitch input commanded to the OTT and the resultant pressure response at the pressure transducer location just mentioned. Although a theoretical step input consists of an infinite slope where the step occurs, a physically realizable step input, such as that commanded by the OTT, will be limited by the pitch inertia, stress, and load limitations of the model undergoing pitch. As can be seen, a step input that closely approaches a theoretical step input can, in fact, be applied by the OTT. The unsteady pressure measurement is also quite noisy, as can be seen.

Using the sequence of step pitch motions of the OTT as the input and the unsteady pressure measurement as the output, deconvolution is applied to identify the unsteady aerodynamic impulse response. Figure 3 presents the time- and frequency-domain versions of the pressure impulse response identified via deconvolution. As can be seen in Fig. 3. the identified impulse response exhibits significant frequency content, as is to be expected for an impulse response. A large frequency spike can be seen at about 70 Hz, the cause of which is still under investigation. An analysis of the unsteady aerodynamic impulse responses at all pressure transducer locations can provide a spatial mapping of the frequency characteristics of a given configuration at a given test condition. This type of spatial mapping can be useful for the design and optimal placement of various flow control devices.

Upon identification, the unsteady aerodynamic impulse response can then be used to predict the unsteady aerodynamic response caused by any OTT input using convolution and the impulse response of Fig. 3. In the following figures, comparisons are made between predicted unsteady aerodynamic responses and the measured responses for several sinusoidal OTT motions.

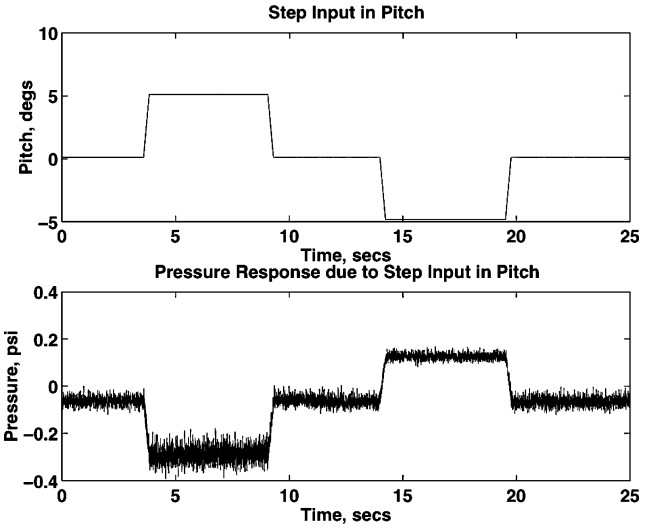

Fig. 2 Commanded pitch motion and resultant pressure response at 30% span and 20% chord at $M = 0.9$, $Q = 150$ psf for the RSM.

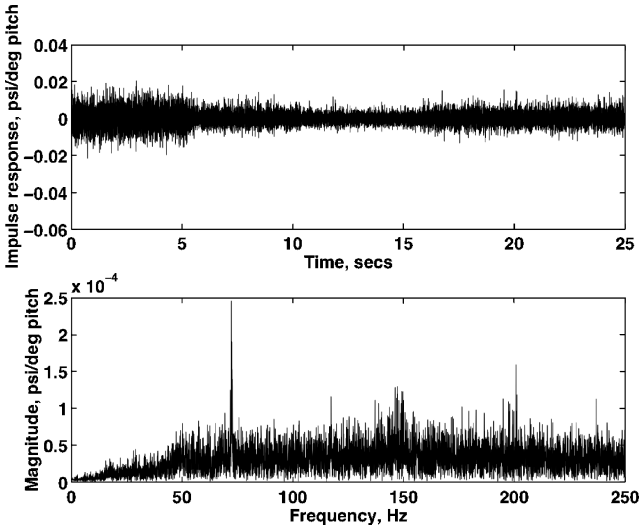

Fig. 3 Pressure impulse response obtained via deconvolution of the commanded OTT input and the resultant pressure response for the RSM; time domain and frequency domain (magnitude).

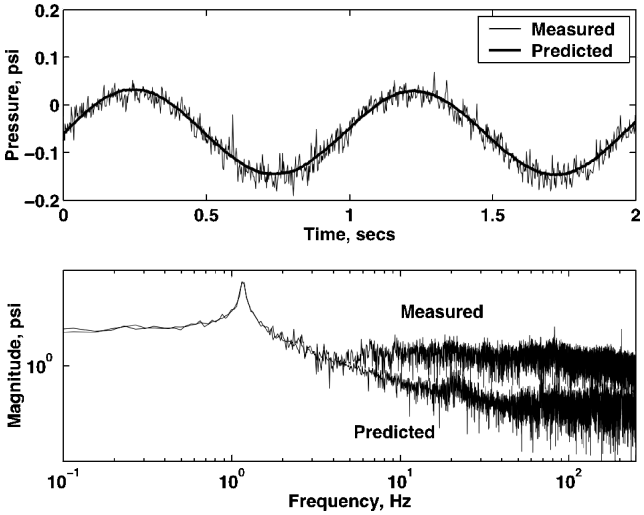

Fig. 4 Measured and predicted pressure responses caused by a 1.2-Hz sinusoidal motion of the OTT for the RSM; time domain and frequency domain (magnitude).

Figure 4 presents the comparison between the measured pressure response and the corresponding predicted pressure response for a commanded oscillation of 1.2 Hz. The comparison is excellent and demonstrates the ability of the method to capture the dominant (driving) frequency while filtering out uncorrelated noise. The filtering is applied uniformly to both low and high uncorrelated frequencies. This precludes the need for low-pass, high-pass, or bandpass filters for which the analyst would have to select a desired frequency range for filtering. However, that desired frequency range might not be evident.

Figure 5 presents the comparison between the measured pressure response and the corresponding predicted pressure response for a commanded oscillation of 5.1 Hz. Again, the method clearly identifies the correct frequency component for this pressure measurement along with good filtering of the noise.

Figure 6 presents the comparison between the measured pressure response and the corresponding predicted pressure response for a commanded oscillation of 8.2 Hz. At this frequency, some higher-frequency content begins to appear in the predicted response as well.

Figure 7 presents the comparison between the measured pressure response and the corresponding predicted pressure response for a commanded oscillation of 10.1 Hz. For this case, without the predicted response it would be very difficult to discern any periodicity

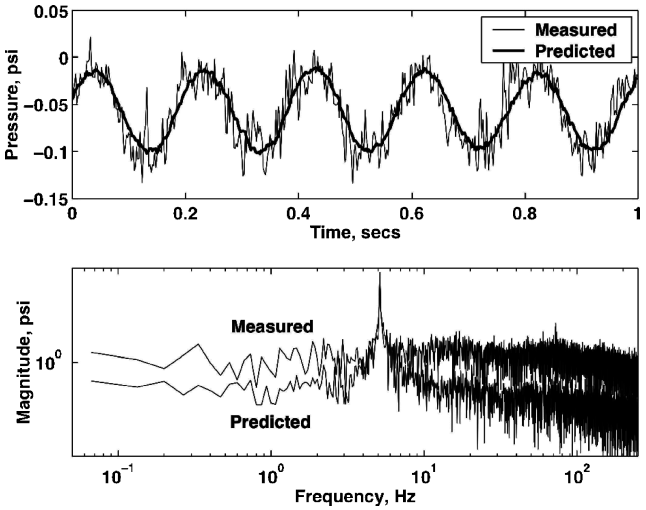

Fig. 5 Measured and predicted pressure responses caused by a 5.1-Hz sinusoidal motion of the OTT for the RSM; time domain and frequency domain (magnitude).

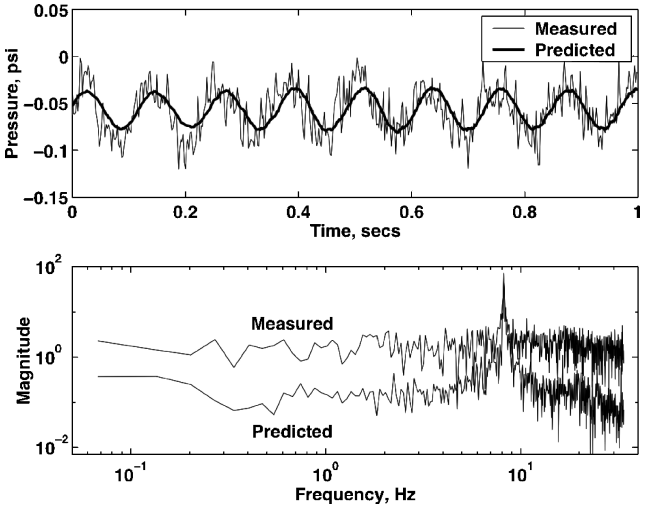

Fig. 6 Measured and predicted pressure responses caused by a 8.2-Hz sinusoidal motion of the OTT for the RSM; time domain and frequency domain (magnitude).

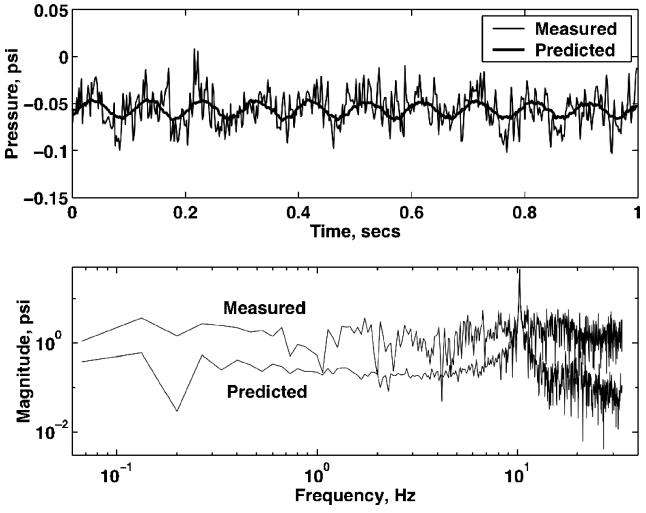

Fig. 7 Measured and predicted pressure responses caused by a 10.1-Hz sinusoidal motion of the OTT for the RSM; time domain and frequency domain (magnitude).

in the measured response. The filtering capability of the deconvolution method proves to be essential at this frequency.

At this condition, the linearity of the measured pressure responses (for this pressure transducer location) is defined by the excellent correlation between the experimental results and the results computed using convolution. If predicted results do not compare well with measured results, this could be an indication that some nonlinearity has influenced the measured response.

In addition, because deconvolution involves input/output correlation any uncorrelated white noise (measurement noise) is easily filtered out. Note that for several of the examples presented, the filtering was applied at all uncorrelated frequencies, both low and high frequencies. Simple low-pass or high-pass filters would not be able to match this level of filtering capability, and much more sophisticated bandpass filters would have to be introduced. However, even with bandpass filters the question of which frequency range to filter would remain a serious question for the analyst. Deconvolution automatically handles the filtering without a priori definition of a frequency range where filtering is desired. Analysis of these results can subsequently be used to identify regions of linear and nonlinear behavior, which will be helpful in understanding dominant flow physics.

BSCW/OTT Results

For the BSCW on the OTT, results are presented for pressure measurements at the trailing edge, at a Mach number of 0.5, a dynamic pressure of 150 psf, and zero-deg angle of attack.

Presented in Fig. 8 is the unsteady aerodynamic impulse response identified via deconvolution, both in the time and frequency domain. From Fig. 8, the response (for this condition and this position on the airfoil) appears fairly flat at lower frequencies with increasing content at higher frequencies. Again, comparison of unsteady aerodynamic impulse response functions for a given configuration at several conditions and at several pressure ports can be useful in identifying dominant flow physics and the frequency range at which these phenomena occur. The important point to be made in this paper is that these functions (unsteady aerodynamic impulse responses) exist and can be identified for any configuration.

Figure 9 presents the measured and predicted pressure responses caused by a 1-Hz sinusoidal motion of the OTT in the time domain and frequency domain (magnitude). Again, the comparison is very good and demonstrates the ability of the method to capture the dominant (driving) frequency while filtering out uncorrelated noise. Once again, the filtering is applied uniformly to both low and high uncorrelated frequencies.

Figure 10 presents the measured and predicted pressure responses caused by a 2-Hz sinusoidal motion of the OTT in the time domain

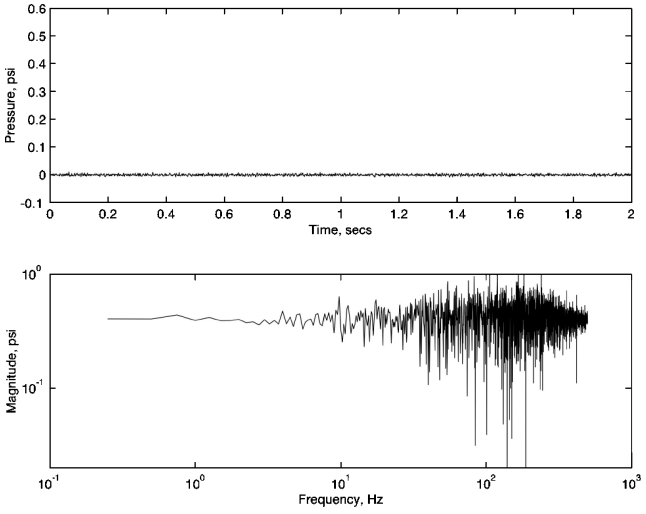

Fig. 8 Pressure impulse response obtained via deconvolution of the commanded OTT input and the resultant pressure response for the BSCW at the trailing edge; time domain and frequency domain (magnitude).

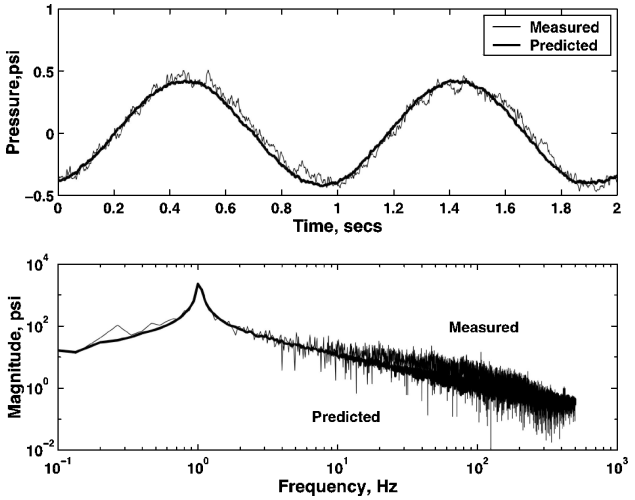

Fig. 9 Measured and predicted pressure responses caused by a 1-Hz sinusoidal motion of the OTT for the BSCW; time domain and frequency domain (magnitude).

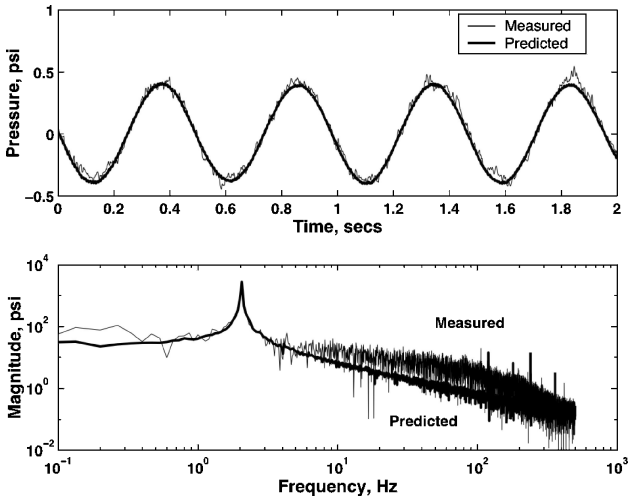

Fig. 10 Measured and predicted pressure responses caused by a 2-Hz sinusoidal motion of the OTT for the BSCW; time domain and frequency domain (magnitude).

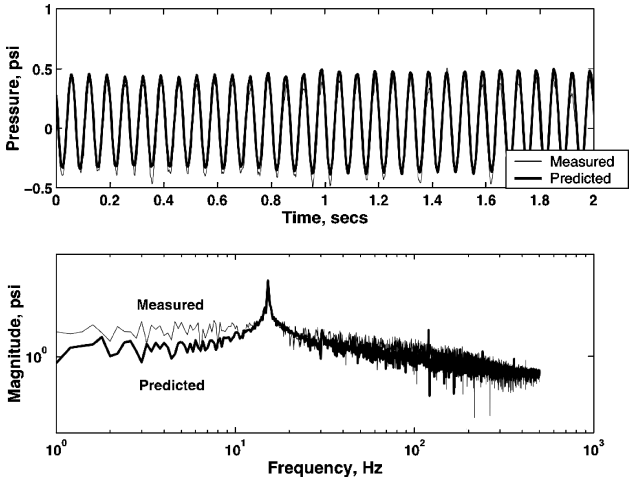

Fig. 11 Measured and predicted pressure responses caused by a 15-Hz sinusoidal motion of the OTT for the BSCW; time domain and frequency domain (magnitude).

and frequency domain (magnitude). The comparison is very good with excellent filtering of the uncorrelated noise.

Finally, Fig. 11 presents the measured and predicted pressure responses caused by a 15-Hz sinusoidal motion of the OTT in the time domain and frequency domain (magnitude). For this case the comparison is good, but Fig. 11 indicates an asymmetry in the measured response not captured by the predicted response. Additional analyses are required to determine if this difference is caused by a possible nonlinear effect. Although at this subsonic Mach number, nonlinear aerodynamic effects are not expected in general, because this pressure measurement is at the trailing edge, some local flow separation induced by the higher-frequency oscillations can be occuring.

Conclusions

A method for the identification of experimental aerodynamic impulse responses has been presented. The results verify the existence of these functions in an experimental setting. The results presented included applications of the method to unsteady aerodynamic (pressure) responses for two wind-tunnel models: a rigid semispan model and a benchmark supercritical wing. The method was used to successfully predict the pressure responses caused by various sinusoidal oscillations for both wind-tunnel models. An added bonus of the method is its ability to filter out uncorrelated white noise from noisy measurements. The method can, therefore, be used to 1) identify the level of linearity for a given measurement and 2) filter out the noise from experimental measurements. Additional analyses are required to 1) further investigate the value of spatial frequency mappings for a given configuration and 2) use the information provided by this method to gain insight into the dominant flow physics. These results represent the first time that experimental unsteady aerodynamic impulse responses have been successfully identified.

References

[1]Silva, W. A., Keller, D. F., Florance, J. R., Cole, S. R., and Scott, R. C., "Experimental Steady and Unsteady Aerodynamic and Flutter Results for HSCT Semispan Models," AIAA Paper 2000-1697, April 2000.

[2]Piatak, D. J., and Cleckner, C. S., "A New Forced Oscillation Capability for the Transonic Dynamics Tunnel," AIAA Paper 2002-0171, Jan. 2002.

[3]Murphy, P. C., and Klein, V., "Estimation of Aircraft Unsteady Aerodynamic Parameters form Dynamic Wind Tunnel Testing," AIAA Paper 2001-2975, Aug. 2001.

[4]Scott, R. C., Silva, W. A., Keller, D. F., and Florance, J. R., "Measurement of Unsteady Pressure Data on a Large HSCT Semispan Wing and Comparison with Analysis," AIAA Paper 2002-1648, April 2002.

[5]Parekh, D. E., and Glezer, A., "AVIA: Adaptive Virtual Aerosurface," AIAA Paper 2000-2474, June 2000.

[6]Honohan, A. M., Amitay, M., and Glezer, A., "AIVA: Adaptive Virtual Aerosurface," AIAA Paper 2000-2401, June 2000.

[7]Chatlynne, E., Rumigny, N., Amitay, M., and Glezer, A., "Virtual Aero-Shaping of a Clark-Y Airfoil Using Synthetic Jet Actuators," AIAA Paper 2001-0732, Jan. 2001.

[8]Amitay, M., Horvath, M., Michaux, M., and Glezer, A., "Virtual Aerodynamic Shape Modification at Low Angles of Attack Using Synthetic Jet Actuators," AIAA Paper 2001-2975, June 2001.

[9]Lucia, D. J., Beran, P. S., and Silva, W. A., "Reduced-Order Modeling: New Approaches for Computational Physics," *Journal of Progress in Aerospace Sciences*, Vol. 40, No. 1–2, 2004, pp. 51–117.

[10]Silva, W. A., and Bartels, R. E., "Development of Reduced-Order Models for Aeroelastic Analysis and Flutter Prediction Using the CFL3Dv6.0 Code," *Journal of Fluids and Structures*, Vol. 19, No. 6, 2004, pp. 729–745.

[11]Bennett, R. M., Eckstrom, C. V., Rivera, J. A., Dansberry, B. E., Farmer, M. G., and Durham, M. H., "The Benchmark Aeroelastic Models Program-Description and Highlights of Initial Results," NASA TM-104180, Dec. 1991.

[12]Dansberry, B. E., Durham, M. H., Bennett, R. M., Rivera, J. A., Silva, W. A., and Wieseman, C. D., "Experimental Unsteady Pressures at Flutter on the Supercritical Wing Benchmark Model," AIAA Paper 93-1592, April 1993.

[13]Silva, W. A., "Identification of Nonlinear Aeroelastic Systems Based on the Volterra Theory: Progress and Opportunities," *Journal of Nonlinear Dynamics*, Vol. 39, No. 1–2, 2005, pp. 25–62.

[14]Hajj, M. R., and Silva, W. A., "Nonlinear Flutter Aspects of the Flexible High-Speed Civil Transport Semispan Model," *Journal of Aircraft*, Vol. 41, No. 5, 2004, pp. 1202–1208.